mathematics

MDPI

Article

Minimization of Torque Ripples in Multi-Stack Slotted Stator Axial-Flux Synchronous Machine by Modifying Magnet Shape

Zia Mahmood [1], Junaid Ikram [1], Rabiah Badar [1], Syed Sabir Hussain Bukhari [2,*], Madad Ali Shah [2], Ali Asghar Memon [3] and Mikulas Huba [4,*]

[1] Department of Electrical and Computer Engineering, COMSATS University Islamabad, Islamabad 45550, Pakistan; ziamehmood@gmx.com (Z.M.); junaidikram@comsats.edu.pk (J.I.); rabiah.badar@gmail.com (R.B.)
[2] Department of Electrical Engineering, Sukkur IBA University, Sukkur 65200, Pakistan; madad@iba-suk.edu.pk
[3] Department of Electrical Engineering, Mehran University of Engineering and Technology, Jamshoro 76062, Pakistan; ali.asghar@faculty.muet.edu.pk
[4] Institute of Automotive Mechatronics, Faculty of Electrical Engineering and Information Technology, Slovak University of Technology in Bratislava, 81219 Bratislava, Slovakia
* Correspondence: sabir@iba-suk.edu.pk (S.S.H.B.); mikulas.huba@stuba.sk (M.H.)

Abstract: This paper presents a proposed model of a multi-stack slotted stator axial-flux type permanent magnet synchronous machine (AFPMSM) specifically for reducing torque ripple. The proposed AFPMSM model uses pentagon-shaped permanent magnets (PMs). It has a low value of cogging torque and torque ripples compared to the conventional model with a trapezoidal magnet shape. Additionally, it has increased internal generated voltage (Ef) as compared to the conventional model. To further enhance Ef phases and minimize cogging torque of the proposed model, the proposed AFPMSM model was optimized by varying different sides of PMs using a genetic algorithm (GA). A time-stepped three-dimensional (3D) finite element analysis (FEA) was performed for the comparative analysis of conventional, proposed, and optimized AFPMSM models. From this comparative performance analysis, it is observed that torque ripples and cogging torque of the optimized AFPMSM are significantly decreased, while output average torque is appreciably increased. Ef and output power are also enhanced.

Keywords: axial-flux machine; pentagon magnet shape; torque ripple; internal generated voltage

MSC: 18B20

Citation: Mahmood, Z.; Ikram, J.; Badar, R.; Bukhari, S.S.H.; Ali Shah, M.; Memon, A.A.; Huba, M. Minimization of Torque Ripples in Multi-Stack Slotted Stator Axial-Flux Synchronous Machine by Modifying Magnet Shape. *Mathematics* **2022**, *10*, 1653. https://doi.org/10.3390/math10101653

Academic Editors: Vladimir Prakht, Mohamed N. Ibrahim and Anton Dianov

Received: 28 March 2022
Accepted: 5 May 2022
Published: 12 May 2022

1. Introduction

Recently, power generation using the kinetic energy of wind has gained popularity because it is renewable, widely available, eco-friendly, and cost-effective once installed. The generators generally used in windmills include synchronous generators (SGs), induction or asynchronous generators (IGs), radial-flux type permanent magnet synchronous generators (RFPMSGs), and axial-flux type permanent magnet synchronous generators (AFPMSGs) [1–4]. The AFPMSM can be used for various applications such as wind power, electric vehicle, lifts, ship propulsion, drills, blowers, and escalators. At low rotational speed power generation, the AFPMSM has the advantage of high efficiency in comparison to other generators. This is due to the disc-shaped structure of the AFPMSM [5–8]. The use of the AFPMSM reduces the system complexities since without using the gearbox power can be generated at the low speed.

As compared to other topologies of AFPMSMs, the slotted stator type has the benefit of high-power density as well as high torque as the air gap between the rotor and the stator is reduced. The slotted stator AFPMSM has one distinct advantage over other topologies of AFPPMSM in that for the same power output it requires magnets of less volume. Therefore,

the slotted AFPMSM reduces the cost of the magnets and also reduces the weight of the machine [9,10]. The slotted stator AFPMSM has better mechanical stability due to its robust structure, and it has a uniform force of attraction between the rotor and the stator [11–13].

The minimization of torque ripple is necessary for the smooth operation of the slotted stator AFPMSM. However, the slotted stator AFPMSM produces torque ripples in a similar way to all the other AFPMSMs. In the slotted stator AFPMSM, the categories of torque ripple can be classified as follows: cogging torque, saturation in magnetic core, and non-sinusoidal Ef [14,15]. Several different techniques, such as the ratio of pole width to pole pitch, magnet shaping (trapezoidal, circular, rectangular, etc.), different winding types (such as ring and drum) and coil shapes, sloth skewing, magnet skewing, dummy slots, magnet overhang, and tooth shaping such as splitting the tooth, have been used for elimination of torque ripples in AFPMSM machines [16–25].

Performance improvement of these machines requires minimization of flux called flux leakage and maximization of air gap flux. The minimization of leakage flux and maximization of air gap flux in RFPM type machines is achieved by arranging the PM in a configuration with some overhang effect [26–28]. Several overhang configuration techniques, including PM overhang in the tangential direction and optimizing the rotor overhang variation, have been proposed for improving the performance and overall efficiency of the AFPM machine [29–31].

In this paper, for the minimization of torque ripples, a topology of the slotted stator AFPMSM with pentagon-shaped PM is proposed. The proposed AFPMSM's cogging torque is greatly reduced by the use of the pentagon-shaped PM in comparison to the conventional model. In order to further reduce the cogging torque of the proposed model, optimization of the proposed magnet was carried out by using varying magnet side lengths. The results were obtained by Latin hypercube sampling (LHS) based on a design variable selected for optimization of the magnet. The objective function and constraints were approximated using the kriging method, and lastly, a heuristic search technique, the genetic algorithm (GA), was utilized in obtaining the optimized results. A time-stepped 3D FEA was utilized for performance analysis of the slotted stator AFPMSM. Three-dimensional FEA was employed because it is highly accurate as compared to other analysis techniques such as analytical modelling and 2D FEA. The remainder of the paper is structured as follows: Section 2 contains an introduction to the conventional and proposed slotted stator AFPMSM models and their performance comparison. This section is followed by Section 3, which involves the process used for the optimization of the proposed magnet and includes its results. In Section 4, the conclusion of the overall research is presented.

2. Proposed Model

This section describes the proposed magnet shape and design of the proposed magnet shape of the slotted stator AFPMSM and gives a comparison of the conventional and proposed models in detail. AFPMSM, which has the trapezoidal-shaped PM, is the conventional model, and AFPMSM, which has the proposed tri right-angle pentagon-shaped PM, is the proposed model. The PMs of both the conventional AFPMSM and the proposed AFPMSM models have a flat surface.

2.1. Proposed Magnet

The proposed magnet is presented in Figure 1. The proposed magnet is called a tri right-angle pentagon-shaped magnet. This is because the proposed magnet has three corners that have an angle of 90 degrees and five sides. The proposed tri right-angle pentagon-shaped magnet has the same volume and the same axial height (thickness) as that of the conventional trapezoidal-shaped magnet. The volume of the proposed magnet is kept the same as that of the conventional magnet by varying the different sides of the proposed magnet, while the thickness is not altered. The sides varied in making the volume of the proposed magnet the same as that of the conventional magnet include the outer pole arc, the active length, and the inner pole arc.

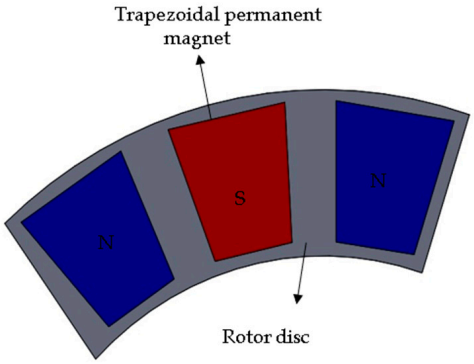

(**a**)

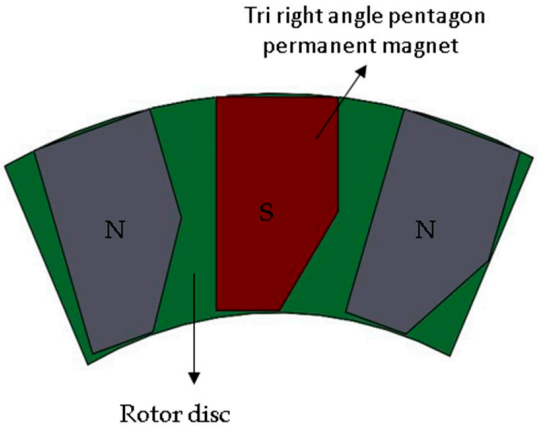

(**b**)

Figure 1. PM shapes: (**a**) trapezoidal, (**b**) tri right-angle pentagon.

The conventional trapezoidal magnets are usually skewed to reduce the cogging torque, while the proposed magnet has built-in some skew effect as shown in Figure 2. Furthermore, keeping the asymmetrical gap between magnets is another cogging torque reduction technique. The gap between adjacent magnets in the conventional model is constant, while in the proposed model the gap between magnets varies as shown in Figure 3.

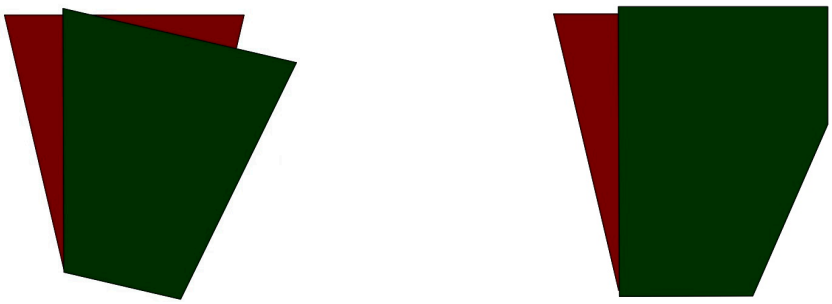

(**a**) (**b**)

Figure 2. (**a**) Conventional magnet skew, (**b**) proposed magnet built-in skew.

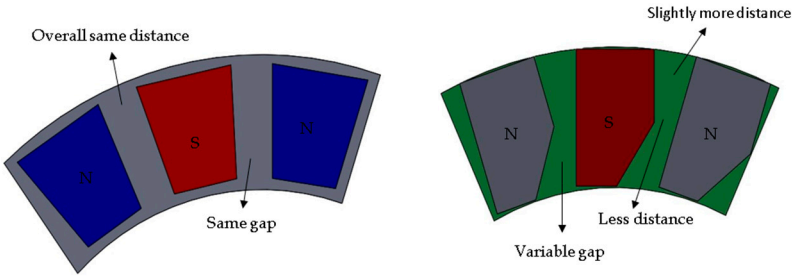

Figure 3. Gap comparison between adjacent magnets: (**a**) conventional magnets, (**b**) proposed magnets.

The proposed magnet has variable distance between the magnets due to which there are some points where the distance between the adjacent magnets is decreased as compared to conventional magnets. This change in distance decreases overall distance between magnets, and permeance of the permanent magnet increases as given by Equation (1)

$$\uparrow P_{Pml} = \frac{\mu_o(D_o - Di)}{\pi} ln\left(1 + \pi \frac{g}{\downarrow d_f}\right) \quad (1)$$

This increase in permanent magnet permeance increases effective permanent magnet permeance given by Equation (2)

$$\uparrow P_{pme} = P_{pm} + 4 \uparrow P_{pml} \quad (2)$$

This increase in permeance reduces air gap flux as shown by Equation (3)

$$\downarrow \phi_g = \frac{1}{1 + \uparrow P_{Pme}/P_g} \phi_r \quad (3)$$

This decrease in the air gap flux decreases the cogging torque of the machine as shown in Equation (4)

$$\downarrow T_{cog} = -\frac{1}{2} \downarrow \Phi_g^2 \frac{dR}{d\theta} \quad (4)$$

where ϕ_g is the air gap flux and $dR/d\theta$ is the change of reluctance with rotor position.

In addition, the proposed magnets have a varying gap between the adjacent magnets due to which their reluctance varies less as compared to the conventional magnets which have a constant air gap. The change of reluctance is greater and abrupt in conventional magnets as represented by Equation (5).

$$\frac{dR}{d\theta}\,(proposed) < \frac{dR}{d\theta}\,(conventional) \quad (5)$$

Therefore, it can be stated that the use of the tri right-angle pentagon-shaped PM in the AFPM machines will reduce cogging torque as well as torque ripple compared to the trapezoidal-shaped PM because the tri right-angle pentagon-shaped PM reduces the flux in the airgap. This reduction in the air gap flux consequently causes a reduction in the overall cogging torque of the machine.

In Section 2.3, the impact of the proposed shape PM on the performance of the AFPMSM is discussed in detail.

2.2. Design of the Slotted Stator AFPMSM

The topology chosen for the design of the slotted stator AFPMSMs consists of dual slotted stators with concentrated winding, a single inner rotor, and a dual outer rotor with back iron. A 25 kW conventional model of the slotted stator AFPMSM was designed. The design process of the slotted stator AFPMSM is shown in Figure 4 in the form of a flow chart. Several different parameters of conventional and proposed slotted stator AFPMSMs

are listed in Table 1. The variables H and N_{ph} represent the height of the PM and the number of turns, respectively. Figure 5 presents an illustration of the design parameters presented in Table 1.

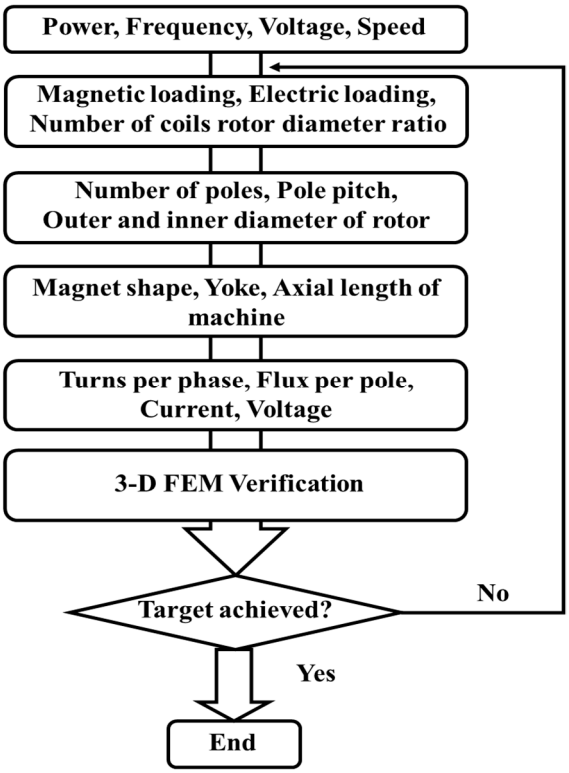

Figure 4. Design process.

Table 1. Conventional AFPMSM and proposed AFPMSM model parameters.

Parameter	Conventional Model	Proposed Model
Rotation	800 rpm	
Number of poles	20	
Number of coils	24	
Connection	star	
Air gap	2 mm	
Rotor yoke height	6 mm	
B_r	1.2 T	
Number of slots	24	
Coil height	9 mm	
N_{ph}	144	
D_o/D_i	296/200 mm	
Volume of PM	6228 mm^3	
Per phase resistance	0.016 ohms	
H	5 mm	
Stator yoke height	11 mm	
Inner tooth width	12.16 mm	
Outer tooth width	24.71 mm	
Slot width	14 mm	
Slot height	14 mm	

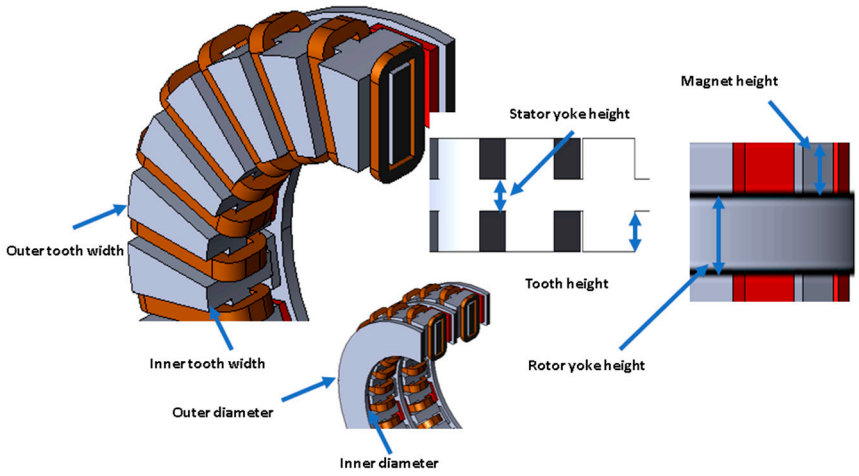

Figure 5. Various design parameters of the AFPMM.

The N_{ph}, D_o, D_i, and B_r variables given in the table represent the number of turns per phase in the machine, the rotor's core outer diameter, the rotor's core inner diameter, and the magnet residual flux density, respectively. Here, it is notable that the height of both the conventional and proposed PM was kept at 5 mm throughout the research. The air gap length of the conventional AFPMSM and proposed AFPMSM models is 2 mm, and the axial length of both the models is the same.

2.3. Comparative Performance Analysis for Conventional AFPMSM and Proposed AFPMSM

In this study, to obtain a precise analysis of different characteristics, time-stepped 3D FEA was utilized, particularly JMAG-Designer ver. 16 tool was used for time-stepped 3D FEA. The comparative performance analysis between the conventional and the proposed AFPMSM models was carried out by keeping the volume of both the conventional as well as the proposed PM the same. In order to keep the volume of the conventional trapezoidal and the proposed tri right-angle pentagon-shaped PMs the same, the height of both the magnets was kept constant while the length of the sides of the proposed magnet was varied. The enhanced view of the conventional and the proposed structure of the slotted stator AFPMSM models is shown in Figure 6.

The air gap flux density of the proposed AFPMSM model is lower compared to the conventional AFPMSM model because in the proposed AFPMSM model the effective permeance of the PM is higher than that in the conventional model, and there is an inverse relationship between air gap flux and effective permeance of the PM. The air gap flux density of the conventional AFPMSM and the proposed AFPMSM model is given in Figure 7.

The three-phase internal generated voltage (Ef) of three phases of both the conventional AFPMSM and proposed AFPMSM are compared in Figure 8. The Ef of the proposed AFPMSM is slightly higher as compared to the Ef of the conventional AFPMSM. An overall increase of 6.4 V_{rms} is achieved in Ef with the proposed AFPMSM model in comparison to the conventional AFPMSM model. This increase in Ef magnitude is obtained due to an increase in the active length of the magnet. A comparison of the active length of the magnet can be seen in Figure 3. The increased active length of the magnet increases the flux linkages of coils which results in the increased internal generated voltage.

The flux density distribution plot of the conventional and proposed models is presented in Figures 9 and 10. The flux density distribution is higher in the central rotor back iron of the conventional and proposed models, whereas the flux density distribution in the outer rotor core and stator core is lower than the central rotor core. The maximum flux density is 2.1 T in the central rotor core, 1.9 T in the outer rotor core, and 1.6 T in the stator core of the conventional model. The maximum flux density distribution is 2.1 T

in the central rotor core, 1.9 T in the outer rotor core, and 1.6 T in the stator core of the proposed model.

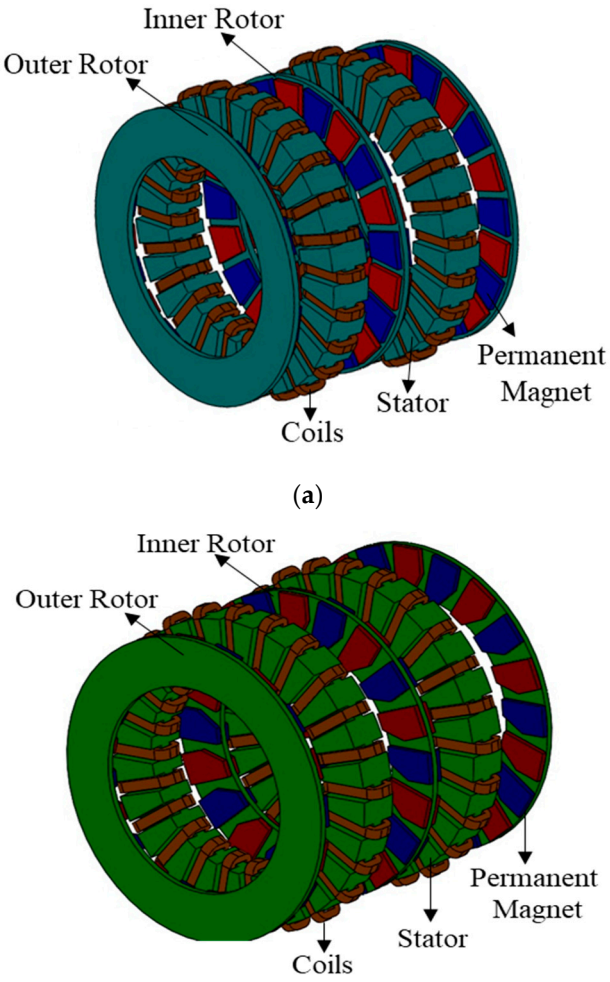

Figure 6. Enhanced view of AFPMSM model with concentrated winding: (**a**) conventional AFPMSM, (**b**) proposed AFPMSM.

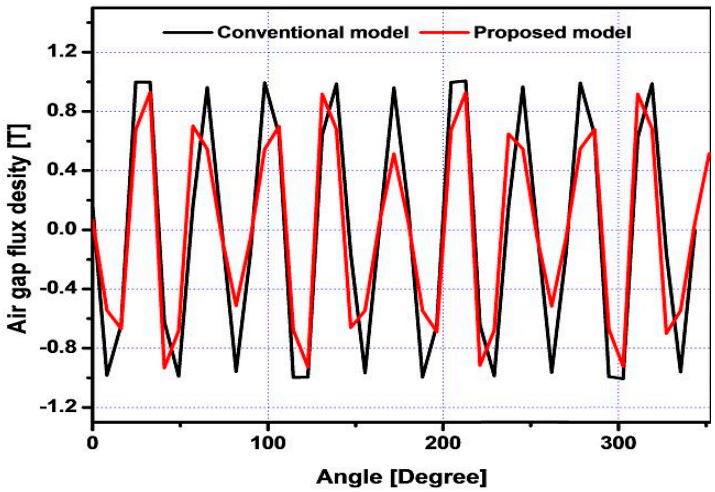

Figure 7. Air gap flux density comparison of conventional AFPMSM and proposed AFPMSM model.

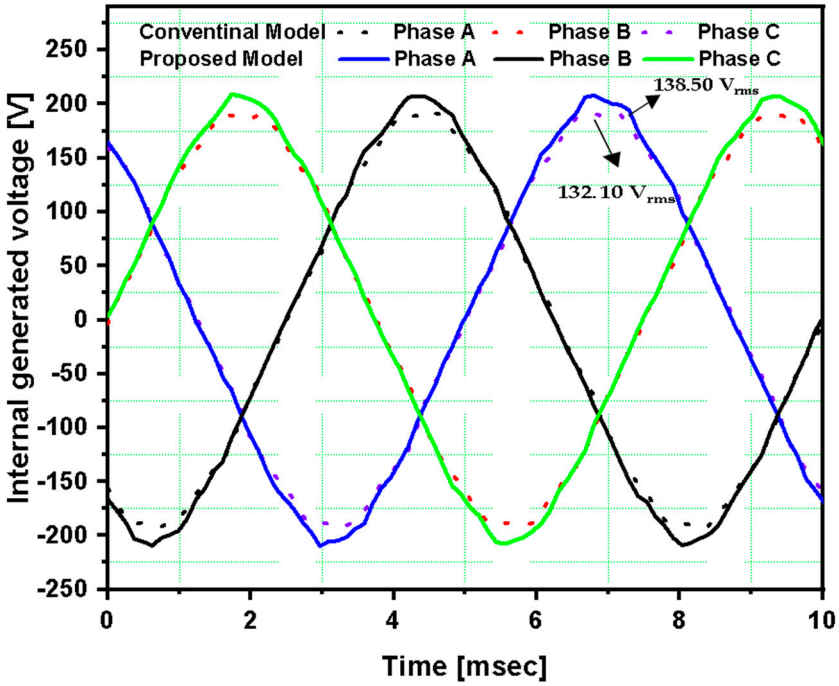

Figure 8. Internal generated voltage analysis of conventional AFPMSM and proposed AFPMSM model.

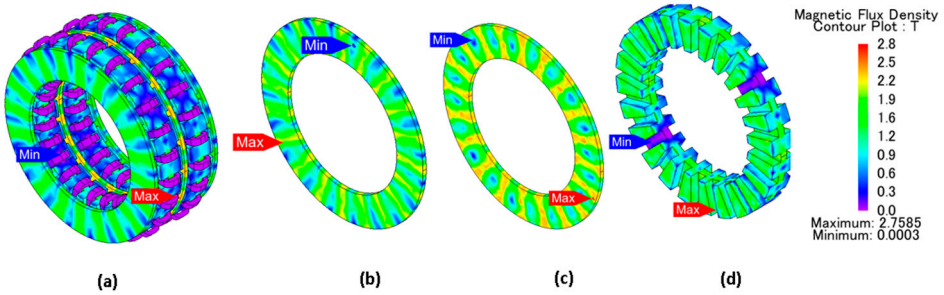

Figure 9. Flux density distribution plot of the conventional AFPMSM model: (**a**) complete model, (**b**) outer rotor core, (**c**) central rotor core, (**d**) stator core.

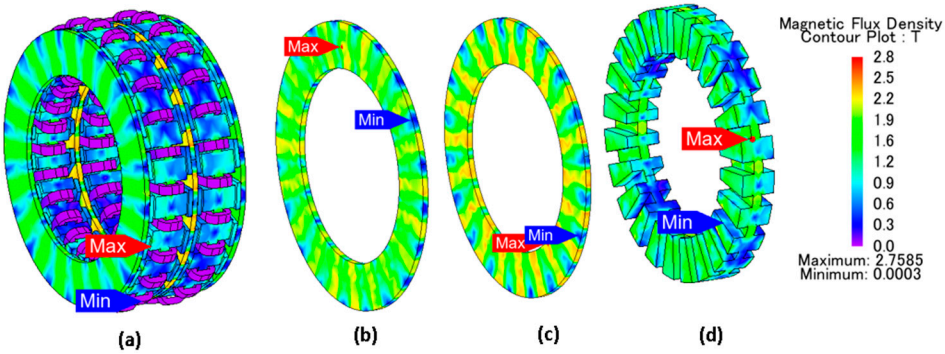

Figure 10. Flux density distribution plot of the proposed AFPMSM model: (**a**) complete model, (**b**) outer rotor core, (**c**) central rotor core, (**d**) stator core.

A comparative cogging torque analysis of the conventional AFPMSM and the proposed AFPMSM model is given in Figure 11. In this analysis, it is observed that with the proposed shape of PM, the cogging torque of the proposed AFPMSM is significantly reduced in comparison to the conventional AFPMSM cogging torque. The use of the proposed PM causes a 34.12 Nm reduction in the peak-to-peak magnitude of cogging torque. The model

with the proposed magnet has an overall 70.3% drop in the cogging torque compared to the cogging torque of the conventional model. This significant drop in the peak-to-peak magnitude of cogging torque of the proposed AFPMSM model results in the decrease in air gap flux which is caused by the usage of the tri right-angle pentagon-shaped PM.

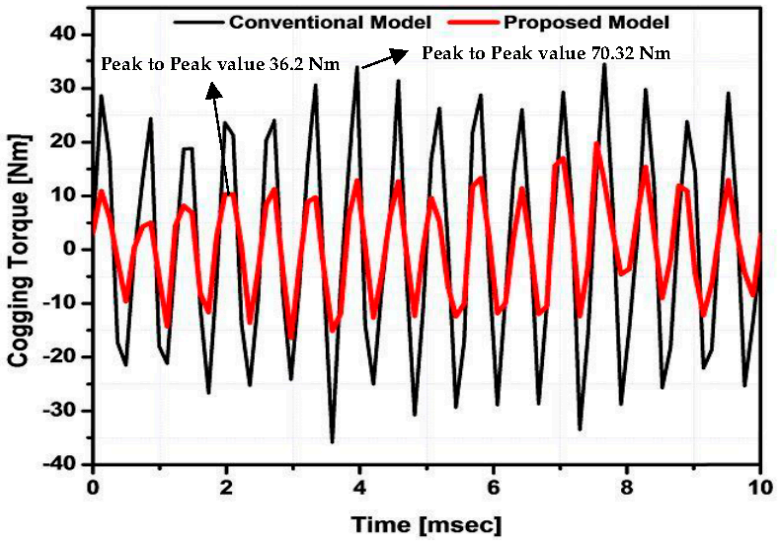

Figure 11. Cogging torque analysis of conventional AFPMSM and proposed AFPMSM model.

The average output torque comparison of both AFPMSM models is given in Figure 12. In the proposed model, the increase in the average output torque is 25.6 Nm. This increase in average output torque value of the proposed AFPMSM model results from the increase in Ef. An overall 60% drop in torque ripples is achieved in the proposed model in comparison to the conventional model. This drop in torque ripples of the proposed model resulted from the drop in the magnitude of cogging torque.

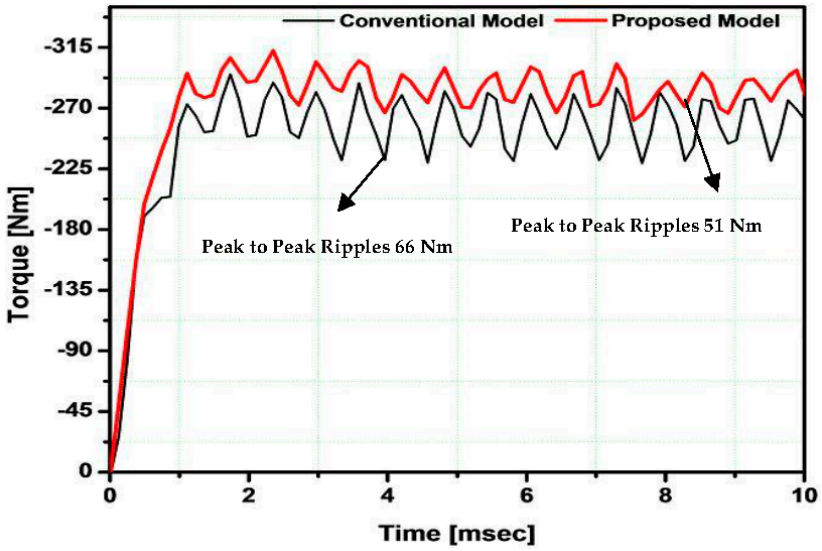

Figure 12. Output torque analysis of the conventional AFPMSM and proposed AFPMSM model.

Table 2 presents a comparison based on performance, between the conventional AFPMSM and the proposed model. Voltage total harmonic distortion of the proposed model is 4.99%, and that of the conventional model is 4.27%. The efficiency of the conventional model is 89.4%, and that of the proposed model is 91.05%.

Table 2. Performance comparison of slotted stator conventional AFPMSM and proposed model.

Parameter	Unit	Conventional Model	Proposed Model
Internal generated voltage (Ef)	V_{rms}	132.10	138.50
Voltage regulation	%	19.97	17.55
V_{THD}	%	4.27%	4.99%
Iron loss	W	2180	1965
Efficiency	%	89.4	91.05
Power (P_{avg})	W	20,029	22,105
Cogging torque (T_{pk2pk})	Nm	70.32	36.2
Torque (T_{avg})	Nm	249.4	275
B_g	T	0.778	0.634

The overall cogging torque and ripples in output torque in the proposed AFPMSM model are much reduced due to the tri right-angle pentagon PM shape and decreased air gap flux. Moreover, the average output torque and V_{rms} of the proposed AFPMSM model increased compared with the conventional AFPMSM model. This increase in average output torque and V_{rms} is due to decreased air gap flux. In order to raise the average output torque of the proposed AFPMSM in comparison to the conventional AFPMSM and to further mitigate the proposed AFPMSM's cogging torque, optimization of the proposed AFPMSM was performed.

3. Optimization

In electrical machines, optimization is often carried out to improve the performance of machines. In order to increase the value of output torque and to reduce the value of the cogging torque compared to the conventional AFPMSM model, optimization of the proposed AFPMSM model was carried out. It is notable that PM volume, as well as height, remained constant during the optimization process.

3.1. Design Variable Selection

Varying magnet side lengths were used to perform optimization and to obtain an optimized AFPMSM model. The inner, as well as the outer radius length of the PM, were varied. The active length of the PM were also varied. PM side length was varied to enhance the flux linking to the coils of the stators. The length of different sides of the PM was varied from the rotor's yoke outer radius to the stator's coil outer radius and from the rotor's yoke inner radius to the stator's coil inner radius.

The selected three design variables for varying the sides of the PM, X_1, X_2, and X_3, the outer pole arc, active length, and inner pole arc of the magnets, respectively, were taken as design variables in order to alter the performance of the generator as shown in Figure 13. LHS was employed to obtain various combinations of the design variables.

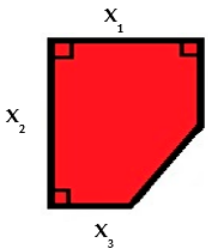

Figure 13. Design variables.

For each combination obtained from LHS, the height and the volume were kept constant, and this is achieved by adjusting the remaining sides of the PM.

3.2. Process of Optimization

The process of optimization of the proposed AFPMSM is shown in Figure 14. In the first step, the design variable and the objective function were selected. The design variables were used to obtain the design experiments. The design experiments were obtained from LHS. On the basis of the design variables, 23 design experiments were obtained. In order to ensure the machine weight constant and for a fair comparison between the proposed and optimized models, the height and the volume of the magnet were kept the same. The performance analysis of all the design experiments was carried out using 3D FEA. After recording the cogging torque and Ef against each design experiment in the form of a table, the objective function was approximated using the kriging method. After the objective function was approximated, a micro genetic algorithm (GA) was employed to obtain optimized values of selected variables.

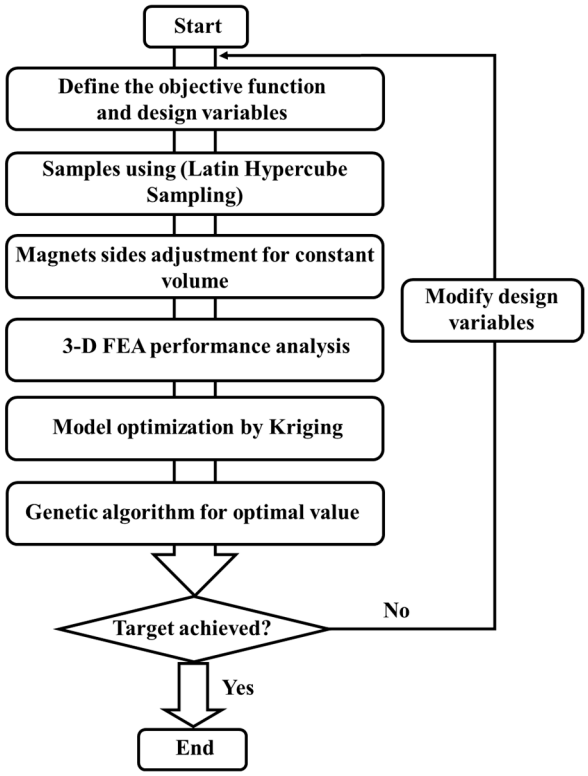

Figure 14. Optimization design process.

When the optimized value of selected variables was obtained, 3D FEA based on the optimal values of the variables was performed in order to validate optimal results of the variables obtained from the GA.

3.3. Results of the Optimized Design

Figure 15 shows the air gap flux density of the optimized model. In this comparative analysis of air gap flux of the proposed and optimized model, it is observed that the optimized model has less air gap flux as compared to the proposed model.

The Ef comparison of the optimized AFPMSM with the proposed AFPMSM model is shown in Figure 16. There is an overall 1.8 V_{rms} increase in Ef of the optimized AFPMSM model as compared to the proposed AFPMSM model's Ef. After optimization of the proposed model, a 6% rise in V_{rms} is obtained.

The comparative cogging torque analysis of the proposed and the optimized model is given in Figure 17. The optimization of the proposed model further resulted in the reduction in cogging torque. The drop in the overall peak-to-peak value of cogging torque

is 8.33 Nm after optimization of the proposed AFPMSM model. This reduction in cogging torque is 20% as compared to the cogging torque of the proposed AFPMSM model.

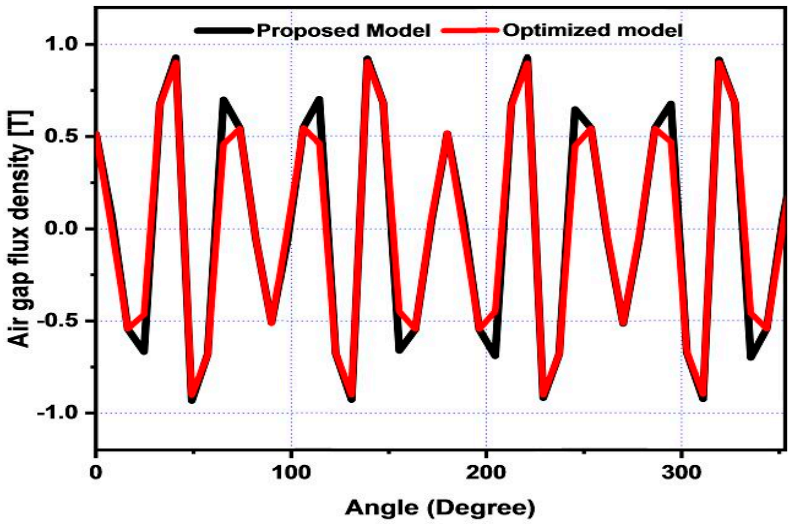

Figure 15. Comparative analysis of air gap flux density of the proposed and the optimized model.

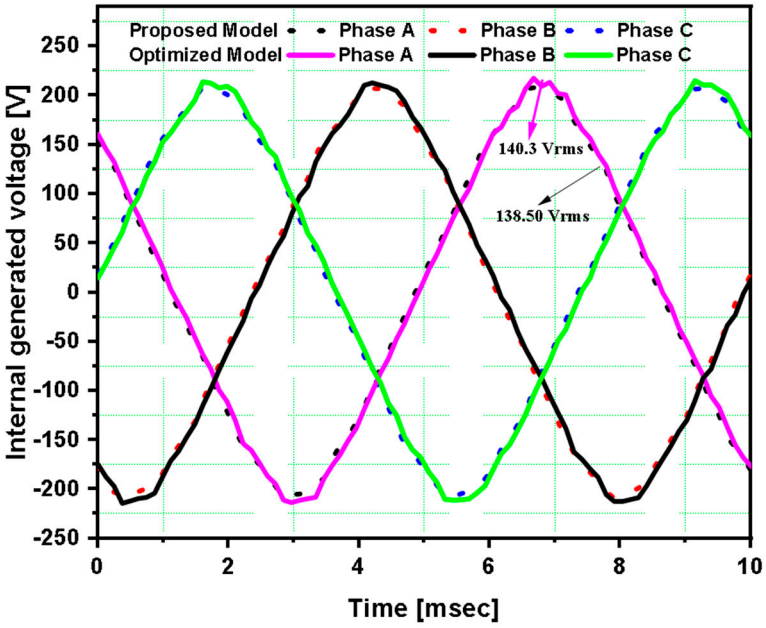

Figure 16. Optimized model internal generated voltage.

The flux density distribution plot of the optimized model is presented in Figure 18. The flux density distribution is higher in the central rotor back iron as compared to the flux density distribution in the outer rotor and stator core. The maximum flux density is 2.1 T in the central rotor core, 1.9 T in the outer rotor core, and 1.6 T in the stator core of the proposed model. The comparison of the average output torque of the proposed and optimized AFPMSM model is given in Figure 19. After optimization, satisfactory enhancement in the average output torque was obtained. The enhancement in average output torque after optimization was 6 Nm, and the torque ripples in the optimized model were also reduced. The optimization also enhanced the output power of the optimized model. The power comparison of the proposed AFPMSM and optimized AFPMSM model reveals that the optimized model has more output power than the proposed model, and this power comparison is given in Figure 20.

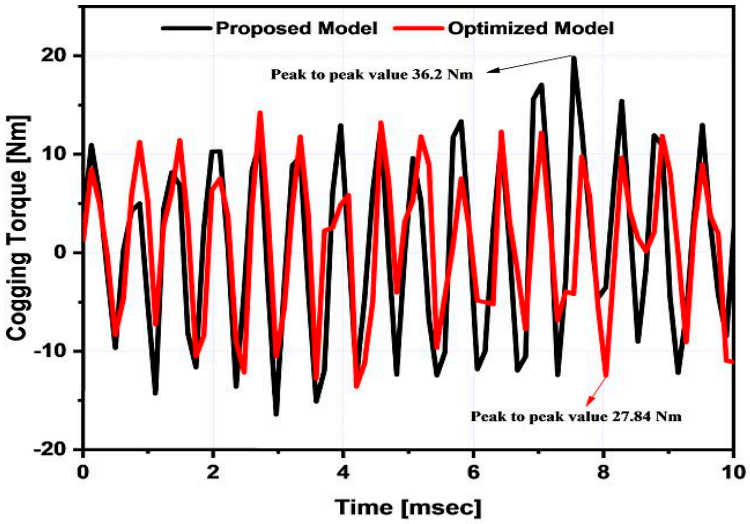

Figure 17. Comparative analysis of the cogging torque of the proposed and optimized models.

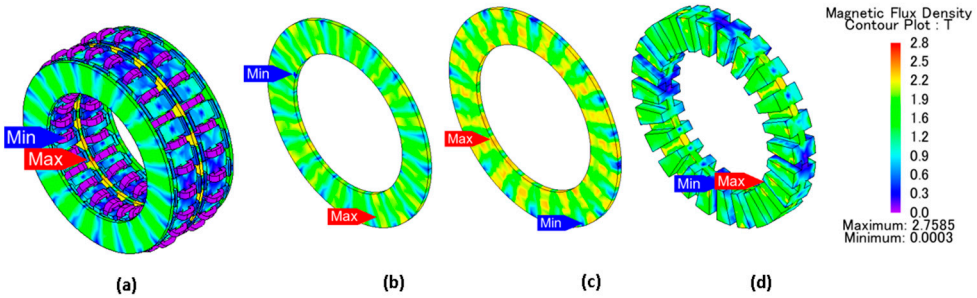

Figure 18. Flux density distribution plot of the optimized AFPMSM model: (**a**) complete model, (**b**) outer rotor core, (**c**) central rotor core, (**d**) stator core.

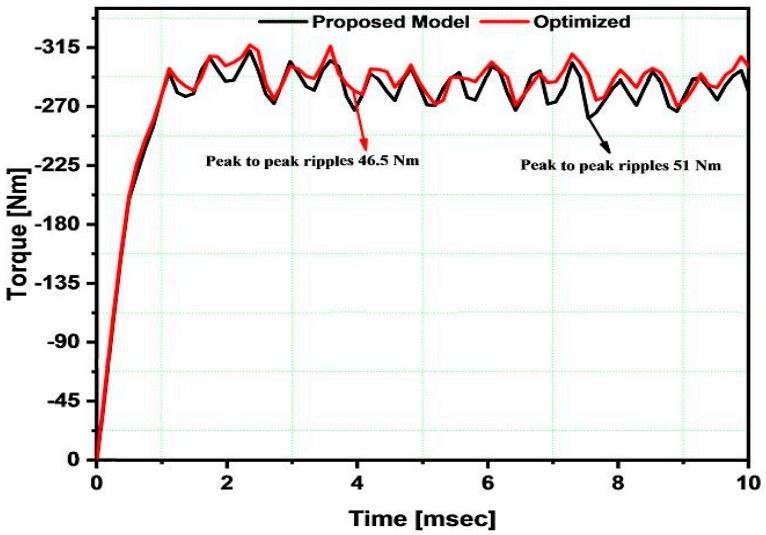

Figure 19. Comparative analysis of output torque of the proposed and optimized models.

In Table 3, several design parameters are presented. The PM in both the proposed and optimized models has the same height and volume for fair performance comparison. The total height of the conventional, proposed, and optimized models in the axial direction is kept the same.

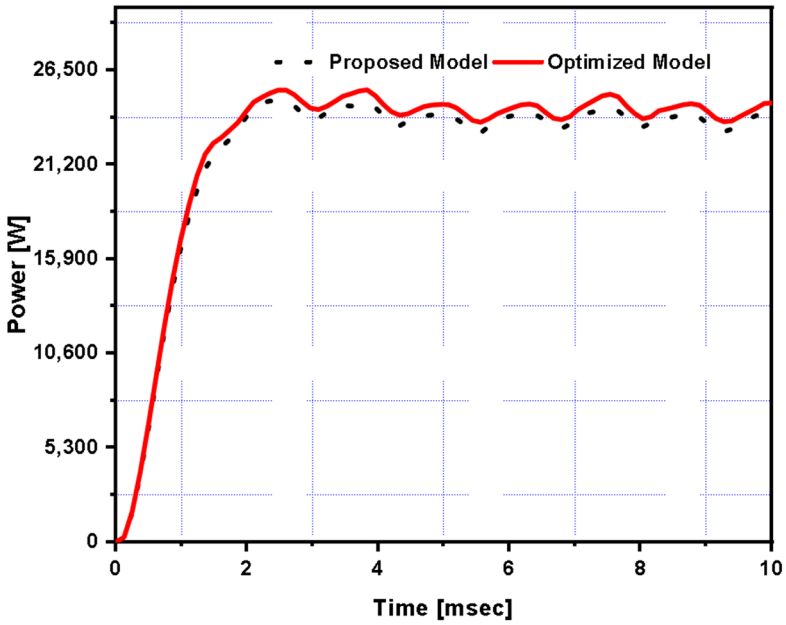

Figure 20. Comparative analysis of output power of the proposed and the optimized models.

Table 3. Proposed and optimized models' various parameters.

Parameter	Unit	Proposed	Optimized
X_1	mm	132.10	48.002
X_2	mm	70.32	28.011
X_3	mm	249.4	15.724
Total height of machine	mm	124	124
Volume of PM	mm^3	6228	6228

In Table 4, the performance comparison of different parameters of the proposed and optimized AFPMSM model is presented. The reduction in peak-to-peak cogging torque is from 70.32 to 36.2 Nm in the proposed AFPMSM model, and this peak-to-peak cogging torque is further reduced from 36.2 to 27.87 Nm after optimization of the proposed magnet is performed. The efficiency of the proposed model is 91.05%, and that of the optimized model is 90.06. This reduction in the efficiency of the optimized model is due to the increased iron loss. The efficiency is reduced at the expense of the increased output torque. Ef is increased from 132.10 to 138.50 V_{rms} in the proposed model and is further increased from 138.50 to 140.3 V_{rms} after the optimization of the proposed model. There is an overall increase in the voltage total harmonic distortion from 4.99% to 6.29%. Therefore, it is pertinent for the voltage total harmonic distortion that the reduction in torque ripple is due to the cogging torque reduction.

Table 4. Comparative analysis of the proposed and optimized models.

Parameter	Unit	Proposed	Optimized
Internal generated voltage (Ef)	V_{rms}	138.50	140.3
Voltage regulation	%	17.04	17.25
V_{THD}	%	4.99%	6.29%
Iron loss	W	1965	2147
Efficiency	%	91.05	90.6
Power (P_{avg})	W	22,105	22,614
Cogging torque (T_{pk2pk})	Nm	36.2	27.87
Torque (T_{avg})	Nm	275	281
B_g	T	0.634	0.588

4. Conclusions

In this paper, a slotted stator AFPMSM model using a flat tri right-angle pentagon PM is proposed. The performance improvement in the AFPMSM model was analyzed by using the proposed flat surface tri right-angle pentagon PM. A comparative analysis of the conventional and proposed models shows that the proposed model has a significantly lower value of cogging torque and has a greatly reduced torque ripple as well as notably increased average torque. The proposed AFPMSM model was then optimized for further reduction in cogging torque. The optimal design of the AFPMSM, obtained after optimization, has reduced torque ripple and a higher value of average output torque when compared to the conventional AFPMSM and the proposed AFPMSM model. Moreover, the optimized model has higher efficiency in comparison with the proposed AFPMSM model. The optimized model of the AFPMSM is better than the conventional and proposed models in terms of Ef, average output torque, torque ripples, and cogging torque. Further reduction in the cogging torque can be achieved by using slotless or coreless configuration at the expense of the decrease in the average power.

Author Contributions: Conceptualization, R.B. and J.I.; methodology, Z.M. and S.S.H.B.; software, Z.M. and S.S.H.B.; writing—original draft preparation, Z.M. and J.I.; writing—review and editing, M.A.S. and A.A.M.; funding acquisition, M.H. All authors have read and agreed to the published version of the manuscript.

Funding: This research was funded by the grant VEGA 1/0745/19 Control and modelling of mechatronic systems in emobility.

Institutional Review Board Statement: Not applicable.

Informed Consent Statement: Not applicable.

Data Availability Statement: Not applicable.

Conflicts of Interest: The authors declare no conflict of interest.

References

1. Snyder, B.; Kaiser, M.J. Ecological and economic cost-benefit analysis of offshore wind energy. *Renew. Energy* **2009**, *34*, 1567–1578. [CrossRef]
2. Panwar, N.L.; Kaushik, S.C.; Kothari, S. Role of renewable energy sources in environmental protection: A review. *Renew. Sustain. Energy Rev.* **2011**, *15*, 1513–1524. [CrossRef]
3. Goudarzi, N.; Zhu, W.D. A review on the development of wind turbine generators across the world. *Int. J. Dyn. Control.* **2013**, *1*, 192–202. [CrossRef]
4. Aakif Baig, M.; Ikram, J.; Iftikhar, A.; Bukhari, S.S.H.; Khan, N.; Ro, J.-S. Minimization of Cogging Torque in Axial Field Flux Switching Machine Using Arc Shaped Triangular Magnets. *IEEE Access* **2020**, *8*, 227193–227201. [CrossRef]
5. Aydin, M.; Huang, S.; Lipo, T.A. Axial flux permanent magnet disc machines: A review. *Conf. Rec. SPEEDAM* **2004**, *8*, 61–71.
6. Chen, Y.; Pillay, P.; Khan, A. PM wind generator topologies. *IEEE Trans. Ind. Appl.* **2005**, *41*, 1619–1626. [CrossRef]
7. Khan, S.; Bukhari, S.S.H.; Ro, J. Design and Analysis of a 4-kW Two-Stack Coreless Axial Flux Permanent Magnet Synchronous Machine for Low-Speed Applications. *IEEE Access* **2019**, *7*, 173848–173854. [CrossRef]
8. Capponi, F.G.; De Donato, G.; Caricchi, F. Recent Advances in Axial-Flux Permanent-Magnet Machine Technology. *IEEE Trans. Ind. Appl.* **2012**, *48*, 2190–2205. [CrossRef]
9. Amin, S.; Khan, S.; Bukhari, S.S.H. A Comprehensive Review of Axial Flux Machines and Its Applications. In Proceedings of the 2nd International Conference on Computing, Mathematics & Engineering Technologies (iCoMET 2019), Sukkur, Pakistan, 30–31 January 2019; pp. 1–7.
10. Hanselman, D.C. *Brushless Permanent Magnet Motor Design*; The Writers' Collective: Cranston, RI, USA, 2003.
11. Xuan, H.V.; Lahaye, D.; Polinder, H.; Abraham Ferreira, J. Influence of stator slotting on the performance of permanent-magnet machines with concentrated windings. *IEEE Trans. Magn.* **2012**, *49*, 929–938. [CrossRef]
12. Kahourzade, S.; Mahmoudi, A.; Ping, H.W.; Uddin, M.N. A Comprehensive Review of Axial-Flux Permanent-Magnet Machines. *Can. J. Electr. Comput. Eng.* **2014**, *37*, 19–33. [CrossRef]
13. El-Refaie, A.M. Fractional-slot concentrated-windings synchronous permanent magnet machines: Opportunities and challenges. *IEEE Trans. Ind. Electron.* **2009**, *57*, 107–121. [CrossRef]
14. Hwang, C.-C.; Li, P.-L.; Chuang, F.; Liu, C.-T.; Huang, K.-H. Optimization for Reduction of Torque Ripple in an Axial Flux Permanent Magnet Machine. *IEEE Trans. Magn.* **2009**, *45*, 1760–1763. [CrossRef]

15. Fei, W.; Luk, P.C.K. Torque ripple reduction of a direct-drive permanent-magnet synchronous machine by material-efficient axial pole pairing. *IEEE Trans. Ind. Electron.* **2011**, *59*, 2601–2611. [CrossRef]
16. Aydin, M.; Zhu, Z.Q.; Lipo, T.A.; Howe, D. Minimization of Cogging Torque in Axial-Flux Permanent-Magnet Machines: Design Concepts. *IEEE Trans. Magn.* **2007**, *43*, 3614–3622. [CrossRef]
17. Ikram, J.; Khan, N.; Khaliq, S.; Kwon, B. Reduction of Torque Ripple in an Axial Flux Generator Using Arc Shaped Trapezoidal Magnets in an Asymmetric Overhang Configuration. *J. Magn.* **2016**, *21*, 577–585. [CrossRef]
18. Gundogdu, T.; Komurgoz, G. Implementation of fractional slot concentrated winding technique in large salient-pole synchronous generators. In Proceedings of the 2012 IEEE Power Electronics and Machines in Wind Applications, Denver, CO, USA, 16–18 July 2012; pp. 1–7.
19. You, Y.-M.; Lin, H.; Kwon, B.-I. Optimal Design of a Distributed Winding Type Axial Flux Permanent Magnet Synchronous Generator. *J. Electr. Eng. Technol.* **2012**, *7*, 69–74. [CrossRef]
20. Xia, B.; Shen, J.-X.; Luk, P.; Fei, W. Comparative Study of Air-Cored Axial-Flux Permanent-Magnet Machines with Different Stator Winding Configurations. *IEEE Trans. Ind. Electron.* **2014**, *62*, 846–856. [CrossRef]
21. El-Hasan, T.S.; Luk, P.C.K. Magnet topology optimization to reduce harmonics in high-speed axial flux generators. *IEEE Trans. Magn.* **2003**, *39*, 3340–3342. [CrossRef]
22. Gieras, J.F.; Wang, R.J.; Kamper, M.J. *Axial Flux Permanent Magnet Brushless Machines*; Kluwer Academic Publishers: Dordrecht, The Netherlands, 2008; pp. 45–60, 92–119.
23. Syed, Q.A.S.; You, Y.-M.; Kwon, B.-I. Design and comparative analysis of single and multi-stack axial flux permanent magnet synchronous generator. *Int. J. Appl. Electromagn. Mech.* **2012**, *39*, 865–872. [CrossRef]
24. Hsieh, M.F.; Dorrell, D.G.; Yeh, Y.H.; Ekram, S. Cogging torque reduction in axial flux machines for small wind turbines. In Proceedings of the 35th Annual Conference of IEEE Industrial Electronics, Porto, Portugal, 3–5 November 2009; pp. 4435–4439.
25. Usman, H.; Ikram, J.; Alimgeer, K.; Yousuf, M.; Bukhari, S.; Ro, J.-S. Analysis and Optimization of Axial Flux Permanent Magnet Machine for Cogging Torque Reduction. *Mathematics* **2021**, *9*, 1738. [CrossRef]
26. Hwang, K.-Y.; Lin, H.; Rhyu, S.-H.; Kwon, B.-I. A Study on the Novel Coefficient Modeling for a Skewed Permanent Magnet and Overhang Structure for Optimal Design of Brushless DC Motor. *IEEE Trans. Magn.* **2011**, *48*, 1918–1923. [CrossRef]
27. Hendershot, J.R.; Miller, T.J.E. *Design of Brushless Permanent-Magnet Motors*; Magna Physics Publishing: Madison, WI, USA; Oxford University Press: Oxford, UK, 1994; pp. 92–93, 681–722.
28. Kim, K.-C.; Koo, D.-H.; Lee, J. The Study on the Overhang Coefficient for Permanent Magnet Machine by Experimental Design Method. *IEEE Trans. Magn.* **2007**, *43*, 2483–2485. [CrossRef]
29. Koo, M.-M.; Choi, J.-Y.; Park, Y.-S.; Jang, S.-M. Influence of Rotor Overhang Variation on Generating Performance of Axial Flux Permanent Magnet Machine Based on 3-D Analytical Method. *IEEE Trans. Magn.* **2014**, *50*, 1–5. [CrossRef]
30. Jo, Y.W.; Cho, Y.H.; Chun, Y.D.; Koo, D.H. Characteristic analysis on overhang effect in axial flux PM synchronous motors with slotted winding. In Proceedings of the CES/IEEE 5th International Power Electronics and Motion Control Conference, Shanghai, China, 14–16 August 2006; IEEE: Piscataway, NJ, USA, 2006; Volume 3, pp. 1–4.
31. Park, H.J.; Jung, H.K.; Jung, S.Y.; Chae, Y.H.; Woo, D.K. Field reconstruction method in axial flux permanent magnet motor with overhang structure. *IEEE Trans. Magn.* **2017**, *53*, 1–4. [CrossRef]